Stabilization of Calcium Oxyapatites with Lanthanum(III)-Created Anionic Vacancies

A. Serret, M. V. Cabañas, and M. Vallet-Regí*

Departamento Química Inorgánica y Bioinorgánica, Facultad de Farmacia, Universidad Complutense, 28040-Madrid, Spain

Received July 3, 2000. Revised Manuscript Received October 2, 2000

Two series of samples of the system $Ca_{10-x}La_x(PO_4)_6(OH)_y$ ($0 \leq x \leq 2$), have been synthesized by solid-state reaction at high temperature. In this composition range the apatite structure is maintained. Cationic distribution was analyzed by Rietveld refinement of the XRD data, showing a preferential substitution of La(III) ions in the Ca(2) position. The introduction of the trivalent ion provokes the transformation of OH^- to O^{2-} ions. Stable oxy- or oxyhydroxyapatites with numerous anionic vacancies have been synthesized as a function of the lanthanum content or the synthesis conditions.

Introduction

Compounds with the apatite-type structure have been widely studied since they can be used for various applications such as biomaterials,[1] catalysts,[2] ionic exchangers,[3] or luminescent materials.[4,5] Calcium hydroxyapatite, $Ca_{10}(PO_4)_6(OH)_2$, (OHAp), is characterized by a structural complexity arising from the disordering of OH^- ions in *c*-axis columns.[6] Usually, this structure can be described on the basis of the $P6_3/m$ space group where two cationic positions, namely, Ca(1) and Ca(2), can be distinguished (Figure 1). The columnar Ca(1) ions are 9-fold coordinated by oxygen atoms, whereas the Ca(2) ions are 7-fold coordinated, and they are located close to the OH^- ions in the channels of the structure. These Ca(2) ions form two triangles of Ca^{2+} ions rotated by 60° from each other around the *c* axis.

The OHAp can accommodate a large number of different ions in its lattice. Substitutions for calcium ions, phosphate ions, or in hexad axis are numerous and complex.[6] The incorporation of foreign cations in the apatite structure is of considerable interest, because it is expected to change the bulk properties of the apatite. For example, although OHAp is generally accepted as a prototype for the apatitic mineral in calcified tissues, the lattice ions of OHAp are substituted to a considerable extent by other ions.[7] Also, this apatite structure has been used extensively as a host lattice for luminescent ions, rare earths, etc.[8,9]

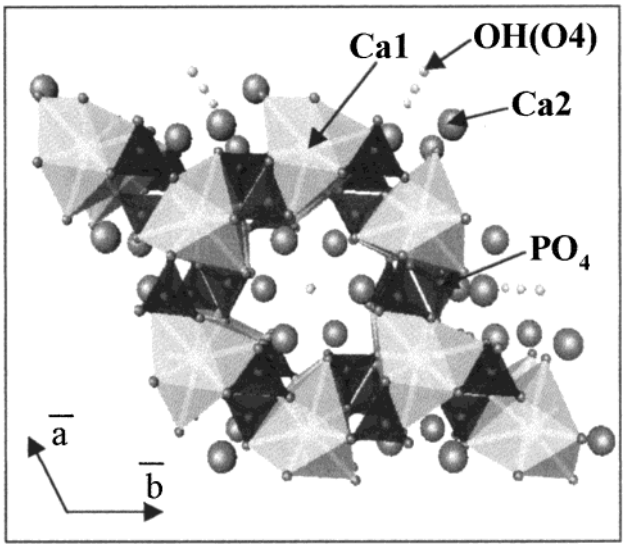

Figure 1. Calcium hydroxyapatite structure along [001] direction (drawing produced with ATOMS, by Shape Software).

On the other hand, it is generally believed that electrical conduction in OHAp is achieved by ionic (proton or hydroxyl ion) transport through the center of the triangle formed by Ca(2) sites along the *c* axis.[10] Vacancies are required for OH^- conduction in order to change positions with OH^- in an electric field. From this point of view, the creation of anionic vacancies in the apatite structure will be interesting. Anionic vacancies have been reported to be produced in the sintering process of OHAp.[11] The maximum number of vacancies would correspond to oxyapatite $Ca_{10}(PO_4)_6O\square$, where $\square$ denotes anionic vacancies. However, this oxyapatite is unstable and rehydrates easily to oxyhydroxyapatite in air.[12]

* To whom correspondence should be addressed. E-mail: Vallet@eucmax.sim.ucm.es. Phone: 34-913941843. Fax: 34-913941786.

(1) Suchanek, W.; Yoshimura, M. *J. Mater. Res.* **1998**, *13*, 94.
(2) Monma, H. *J. Catal.* **1982**, *75*, 200.
(3) Suzuki, T. *Gypsum Lime* **1986**, *204*, 316.
(4) Blasse, G. *Mater. Chem. Phys.* **1987**, *16*, 201.
(5) Tachihante, M.; Zanbon, D.; Cousseins, J. C. *Eur. J. Solid State Inorg. Chem.* **1996**, *33*, 713.
(6) Elliot, J. C. *Structure and Chemistry of the Apatites and Other Calcium Orthophosphates*; Elsevier: Amsterdam, 1994.
(7) LeGeros, R. Z. In *Calcium Phosphates in Oral Biology and Medicine*; Monographs in Oral Science; Myers, H., Ed.; Karger: New York, 1991.
(8) Wanmaker, W. L.; ter Vrugt J. W.; Verlijsdonk J. G. *J. Solid State Chem.* **1971**, *3*, 452.
(9) Toumi, M.; Smiri-Dogguy, L.; Bulou, A. *J. Solid State Chem.* **2000**, *149*, 308.
(10) Takahashi, T.; Tanse, S., Yamamoto, O. *Electrochim. Acta* **1978**, *23*, 369.
(11) Knowles, J. C.; Gross, K.; Berndt, C. C.; Bonfield, W. *Biomaterials* **1996**, *17*, 639.
(12) Trombe, J. C.; Montel, G. *J. Inorg. Nucl. Chem.* **1978**, *40*, 15.

10.1021/cm001117p CCC: $19.00
Published on Web 12/01/2000

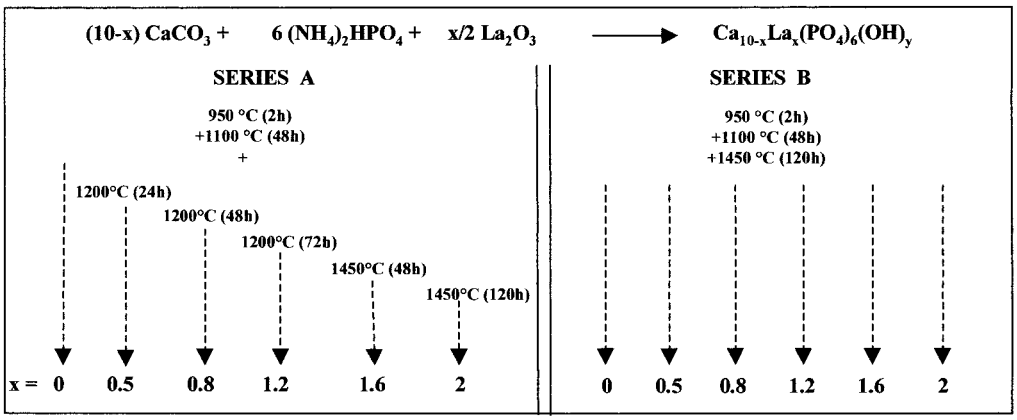

Figure 2. Scheme of the synthesis conditions for samples of series A and B.

To generate anionic vacancies in the apatite structure and to synthesize stable oxy- or oxyhydroxyapatite, in this work Ca^{2+} ions have been substituted by a trivalent ion, La(III). This substitution could be of great interest because two kinds of charge carriers, i.e., OH^- and O^{2-}, may be present in these samples, and a lower activation energy has been reported for O^{2-} conductors (1.5 eV) than for OH^- (2.1 eV) in calcium apatites.[13−15] Hereafter we report the synthesis, structural properties, and cationic distribution of the $Ca_{10-x}La_x(PO_4)_6(OH)_y$ solid solution ($0 \leq x \leq 2$).

Experimental Section

Two series of samples corresponding to the system $Ca_{10-x}La_x(PO_4)_6(OH)_y$ ($0 \leq x \leq 2$) were prepared from stoichiometric amounts of reagent grade $CaCO_3$, $(NH_4)_2HPO_4$, and La_2O_3, by solid-state reaction at high temperature during several days with intermediate grinding. A scheme of the synthesis conditions is displayed in Figure 2.

In **series A**, the samples were synthesized at different temperatures or times, depending on the lanthanum content. To obtain a single phase, as the La content increases, it was necessary to increase the synthesis temperature or time (Figure 2). In **series B**, all the samples were subjected to the same sequence of thermal treatments, 1450 °C during 120 h being the last step of such sequence, which was found necessary to obtain a single phase for $x = 2$ in series A. In both series, the samples were quenched from high temperatures.

Samples were characterized by X-ray diffraction (XRD) in a Philips X'Pert diffractometer by using Cu Kα radiation (C. A. I. Difracción de rayos X. U. C. M.). Fourier transform infrared (FTIR) spectra from 4000 to 400 cm^{-1} of the powdered samples suspended in KBr pellets were recorded with a Nicolet Magna-IR spectrometer 550. High-resolution transmission electron microscopy (HRTEM) and electron diffraction (ED) was performed in all samples using a PHILIPS CM200, FEG electron microscope (C. A. I. Microscopia Electrónica. U. C. M.). Samples for the transmission electron microscopy investigation were prepared by crushing the powder under *n*-butanol and dispersing it over copper grids covered with a holey carbon film.

Results and Discussion

Series A. Figure 3 shows the XRD patterns corresponding to the samples with $x = 0$, 0.5, and 2. The maxima in these patterns are sharp and well resolved and all can be attributed to the hexagonal crystal form of hydroxyapatite on the basis of the space group $P6_3/m$. As the La(III) content increases a progressive change of the intensities and position of the XRD maxima can be observed. The XRD data were analyzed by the Rietveld method. Starting atomic parameters for all refinements came from the refinement performed with neutron data in $P6_3/m$ of Sudarsanan and Young.[16] A pseudo-Voigt function was used to adjust the profile shape. Unit cell and positional parameters, 2θ zero, background parameters, profile, isotropic temperature factor of all the atoms, and occupancy of Ca(1) and Ca(2) positions were allowed to vary.

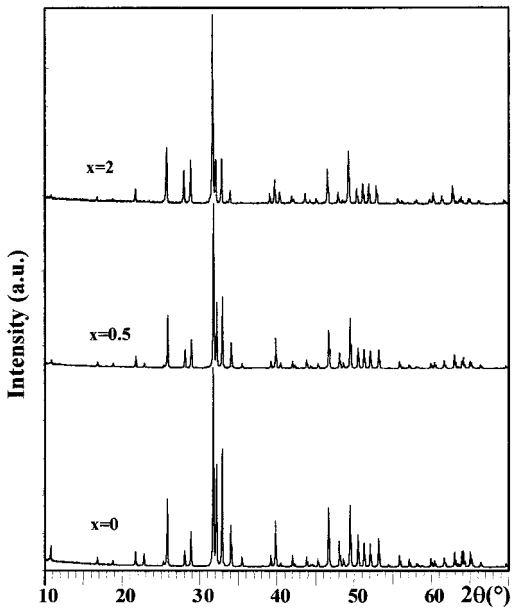

Figure 3. XRD patterns corresponding to series A samples.

The lattice parameters obtained, based on a hexagonal unit cell of the hydroxyapatite, are plotted against lanthanum content in Figure 4. A progressive increase of lattice parameters with increasing La(III) content can be observed. A weighted regression analysis indicates that the change of the cell dimensions with the La content (x) can be described at the 99% confidence level by the equations:

(13) Hartog, H. D.; Welch, D. O.; Royce, B. S. H. *Phys. Status Solidi: B* **1972**, *53*, 201.
(14) Royce, B. S. H. *J. Phys. Suppl.* **1973**, *34*, C9−327.
(15) Yamashita, K.; Owada, H.; Nakagawa, H.; Umegaki, T.; Kanazawa, T. *J. Am. Ceram. Soc.* **1986**, *69*, 590.
(16) Sudarsanan, K.; Young, R. A. *Acta Crystallogr.* **1969**, *B25*, 1534.

Table 1. Occupancy Factors for Ca(1) and Ca(2) Positions as a Function of Lanthanum Content (*x*)[a]

	$x = 0$	$x = 0.5$	$x = 0.8$	$x = 1.2$	$x = 1.6$	$x = 2$
Ca(1) (4f position)[b]	4	4	4	4	4	4
Ca(2) (6h position)	6	5.51(1)	5.18(3)	4.73(3)	4.38(2)	3.99(2)
La (6h position)	0	0.49(1)	0.82(3)	1.27(3)	1.62(2)	2.01(2)
R_B%	8.49	7.35	7.55	7.01	5.63	4.13
R_p%	12.44	11.48	11.06	10.50	11.92	11.30
R_{wp}%	15.81	14.56	14.03	13.70	15.40	14.79

[a] The agreement factors obtained in the Rietveld refinement are also included. [b] 4f and 6h are the Wyckoff notation for the Ca(1) and Ca(2) sublattices, respectively.

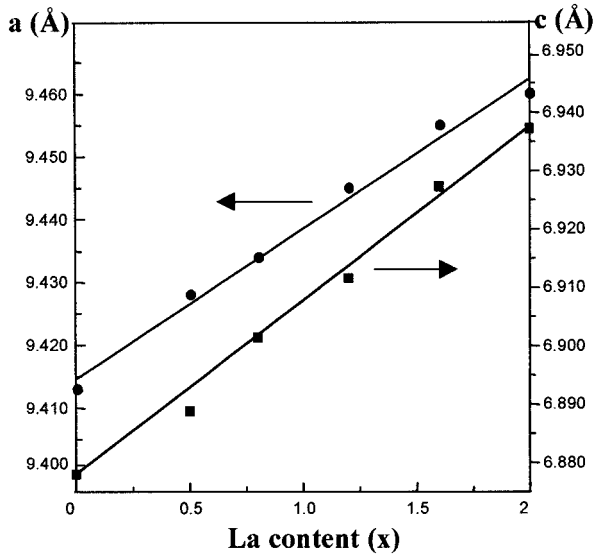

Figure 4. Evolution of cell parameters as a function of lanthanum content.

$$a\ (\text{Å}) = 9.415(1) + 0.0240(1)x \quad \text{and}$$
$$c\ (\text{Å}) = 6.877(2) + 0.030(1)x$$

Taking into account the different scattering factor of the cations involved, the cationic distribution can be studied from XRD data. Initially, the occupancy factor of both Ca(1) and Ca(2) sites was refined. The first refinements show that lanthanum introduction into the structure increases the occupancy factor corresponding to the Ca(2) position, whereas the one corresponding to Ca(1) is close to stoichiometric. That means that La(III) ions occupy only the Ca(2) site of the apatite structure in the entire composition range prepared. In addition, the results obtained (Table 1) show that the experimental occupancy factor values corresponding to lanthanum are in good agreement with the nominal ones (*x*).

When a trivalent cation is introduced into the structure, two possibilities can be considered to keep the charge balance: the creation of cationic vacancies or a transformation of the OH^- to O^{2-} ions. Taking into account that no other phases were observed in the XRD patterns, and the good agreement of occupancy factors with the nominal composition, all the initial calcium must be inside the structure, that means, for the composition range studied, $Ca_{10-x}La_x(PO_4)_6(OH)_y$ ($0 \leq x \leq 2$), the existence of cationic vacancies could be rejected. Then, the substitution of Ca^{2+} by La^{3+} of higher valence must be compensated by the increase of negative charge given by the transformation of OH^- to O^{2-} ions.

Results of XRD data refinements indicate that La^{3+} ions only occupy the Ca(2) sites and that the Ca(1) positions are occupied only by Ca^{2+} ions. Since La^{3+} is somewhat larger than Ca^{2+} (radii of 1.22 and 1.18 Å, respectively),[17] it may be expected that it would fill the larger Ca(1) column sites. However, it is found that the La^{3+} ions fill the Ca(2) sites, then other considerations must be taken into account. When La(III) ions are introduced into the OHAp, a transformation of OH^- to O^{2-} ions occurs. If we consider the structure of hydroxyapatite, this is the oxygen ion that does not belong to any phosphate tetrahedron and it is coordinated triangularly by three cations Ca(2). Then, placing all of the La^{3+} ions in these Ca(2) sites provides for more electrostatic binding and the crystal energy can be lowered by dispersion forces if La^{3+} and O^{2-} ions are nearest neighbors.[18] These results are in agreement with the observations made by other authors that the anion component located in the channels of the structure exerts a marked control on the substitution mechanism and the cationic site occupied.[19,20]

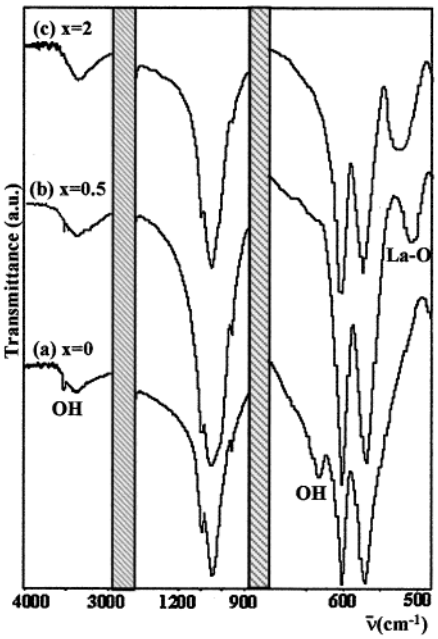

Figure 5. FTIR spectra corresponding to series A samples: (a) $x = 0$, (b) $x = 0.5$, and (c) $x = 2$.

The infrared spectra which correspond to samples with $x = 0$, 0.5, and 2 are shown in Figure 5. (The IR spectra corresponding to the other *x* values are similar to 5c spectrum.) The IR spectra of the samples are typical for apatites with absorption bands in the ranges

(17) Shannon, R. D. *Acta Crystallogr.* **1976**, *A32*, 751.
(18) Schroeder, L. W.; Mathew, M. *J. Solid State Chem.* **1978**, *26*, 383.
(19) Mackie, P. E.; Young, *J. Appl. Crystallogr.* **1973**, *6*, 26.
(20) Fleet, M. E.; Liu, X.; Pan, Y. *J. Solid State Chem.* **2000**, *149*, 391.

960−1100 and 570−610 cm^{-1}, which correspond to the vibration modes of PO_4^{3-} groups of hydroxyapatite.[21] Absorption bands of hydroxyl ions around 3570 and 630 cm^{-1} corresponding to the OH stretching vibration and the OH librational vibration mode, respectively,[21] are observed in sample with $x = 0$; for $x = 0.5$ only a weak band at 3572 cm^{-1} is detected and for higher x values, absorption bands corresponding to hydroxyl ions were not observed. These results show that the substitution of Ca^{2+} by La^{3+} diminishes the number of OH^- ions. In addition, only in the FTIR spectra of the samples with La, an absorption band at 500−525 cm^{-1} attributables to a La−O bond is also displayed. This band appears at 505 cm^{-1} in the sample with $x = 0.5$, whereas in samples with higher La(III) content the band is shifted to 523 cm^{-1}.

It is well know that OHAp dehydrates on heating at high temperatures, according to the following reaction:[12]

$$Ca_{10}(PO_4)_6(OH)_2 \rightarrow Ca_{10}(PO_4)_6(OH)_{2-2y}O_y\square_y + yH_2O \qquad y \leq 1$$

Taking into account the high temperatures used for the synthesis of the samples and according to the XRD and FTIR results, we can say that (1) the samples with $x \leq 0.5$ correspond to oxyhydroxyapatite phase with the following composition

$$Ca_{10-x}La_x(PO_4)_6(OH)_{2+x-2y}O_y\square_{y-x}; \quad y < 1 + x/2; \quad x \leq 0.5$$

and (2) in the samples with $x \geq 0.8$, no OH^- groups were observed in the FTIR spectra. Then for this composition range, only oxyapatite phases are obtained, with a stoichiometry which can be formulated as

$$Ca_{10-x}La_x(PO_4)_6O_y\square_{y-x}; \quad y = 1 + x/2; \quad x \geq 0.8$$

The structural location of the La in the Ca(2) sites, close to the O^{2-} ions in the channel, allows the formation of a La−O bond, which is reflected in an absorption band in the FTIR spectra. This band appears at 505 cm^{-1} for the sample with $x = 0.5$ and it is displaced to higher frequencies (523 cm^{-1}) in samples with higher lanthanum contents. The difference between the sample with $x = 0.5$ and samples with $x > 0.5$ is the existence of OH^- ions in the former. Consequently, the La−O bond is modified by the presence of OH^- ions adjacent to O^{2-} ions. The band displacement from 523 to 505 cm^{-1} in the hydroxylated compound could be related to the existence of a hydrogen bond between neighboring O^{2-} and OH^- ions.[22]

Selected interatomic distances, calculated from atomic positions obtained by the Rietveld method, are given in Table 2. When La(III) ions are introduced into the structure, the average P−O distance decreases slightly from 1.563(4) Å for the nonsubstituted apatite to 1.541(7) Å for the last member, $Ca_8La_2(PO_4)_6O_2$. Regarding the distances corresponding to two independent cation sublattices, the results collected in Table 2 show that the interatomic distances corresponding to the Ca(1) position became slightly shorter as La content increases. However, in the polyhedron corresponding to the Ca(2) site, a progressive increase of the distance Ca(2)−O is observed, except for the interatomic distance Ca(2)−O(4) that decreases when La is introduced. This different behavior between both cationic sites is in accordance with the existence of a preferential substitution site for lanthanum.

Table 2. Selected Interatomic Distances (in Å) as a Function of Lanthanum Content for the Series A Samples

	$x = 0$	$x = 0.5$	$x = 0.8$	$x = 1.2$	$x = 1.6$	$x = 2$
P−O(1)	1.547(4)	1.560(4)	1.597(5)	1.609(6)	1.587(8)	1.574(7)
P−O(2)	1.548(6)	1.559(7)	1.54(1)	1.52(1)	1.54(1)	1.56(1)
P−O(3) × 2	1.579(4)	1.577(4)	1.535(5)	1.526(6)	1.513(1)	1.516(6)
⟨P−O⟩	1.563(4)	1.568(5)	1.552(6)	1.545(7)	1.538(6)	1.541(7)
Ca(1)−O(1)	2.393(3)	2.389(3)	2.357(4)	2.362(1)	2.363(6)	2.364(6)
Ca(1)−O(2)	2.467(3)	2.461(3)	2.478(5)	2.48(1)	2.467(8)	2.487(7)
Ca(1)−O(3)	2.865(3)	2.824(3)	2.815(5)	2.792(6)	2.798(6)	2.799(6)
Ca(2)−O(1)	2.682(3)	2.716(3)	2.743(4)	2.781(4)	2.814(5)	2.855(5)
Ca(2)−O(2)	2.367(6)	2.411(7)	2.462(9)	2.51(1)	2.564(1)	2.52(1)
Ca(2)−O(3)	2.301(4)	2.324(4)	2.368(6)	2.386(7)	2.410(8)	2.436(7)
Ca(2)−O(3)	2.482(3)	2.515(3)	2.549(4)	2.567(5)	2.576(5)	2.576(6)
Ca(2)−O(4)	2.380(3)	2.312(3)	2.240(4)	2.209(5)	2.190(4)	2.143(3)
Ca(2)−Ca(2)	4.052(5)	3.940(4)	3.860(6)	3.796(6)	3.757(5)	3.711(6)

The hydroxyapatite structure can be described as a three-dimensional network of PO_4 tetrahedral with enmeshed columnar Ca(1) ions and with channels passing through it (Figure 1). The introduction of La(III) ions, with an ionic radius slightly higher than that corresponding to Ca(II) ions, originates an elongation of the Ca(2)−O bond lengths. This provokes an increase of the channel size and then a slight decrease in the P−O and Ca(1)−O distances. On the other hand, when La^{3+} ions substitute Ca^{2+} ions, the OH^- ions of the channels (O(4) in Table 2) transform to O^{2-}, which are shifted along the hexad axis toward the center of the triangle formed by the Ca(2) ions, reaching a $z = 0.25$-(3) value for the dioxyapatite. This causes a decrease of the interatomic distance Ca(2)−O(4) and a contraction of the edge length of the triangle, as the La(III) content increases.

The samples were also studied by transmission electron microscopy. The ED patterns along the [001] and [−110] zone axes and the corresponding HRTEM micrographs, for the sample with $x = 2$, are shown in Figure 6. All the ED patterns can be indexed on the basis of an hexagonal apatite phase. No differences and no extra ordering were observed when La ions were introduced into the structure. In addition, the HRTEM migrographs from all the samples show a well-ordered structure without any kind of extended defects. Therefore, we can conclude that lanthanum ions must be randomly distributed into the Ca(2) positions and their introduction does not yield any detectable defects.

Series B. To study the possible thermal stabilization of samples in relation with the La content, and the effect of thermal treatment in the cationic distribution, all the samples were subjected to the same synthesis conditions (Figure 2). The study by XRD (Figure 7) shows that the sample without lanthanum decomposes to $Ca_3(PO_4)_2$, $Ca_2P_2O_7$, and $Ca_4P_2O_9$, according to bibliographic data.[23] However, the samples where La is included in the

(21) Fowler, B. O. *Inorg. Chem.* **1974**, *13*, 194.
(22) Taitai, A.; Lacout, J. L. *J. Phys. Chem. Solids* **1987**, *48*, 629.
(23) Zhou, J.; Zhang, X.; Chen, J.; Zeng, S.; De Groot, K. *J. Mater. Sci.: Mater. Med.* **1993**, *4*, 83.

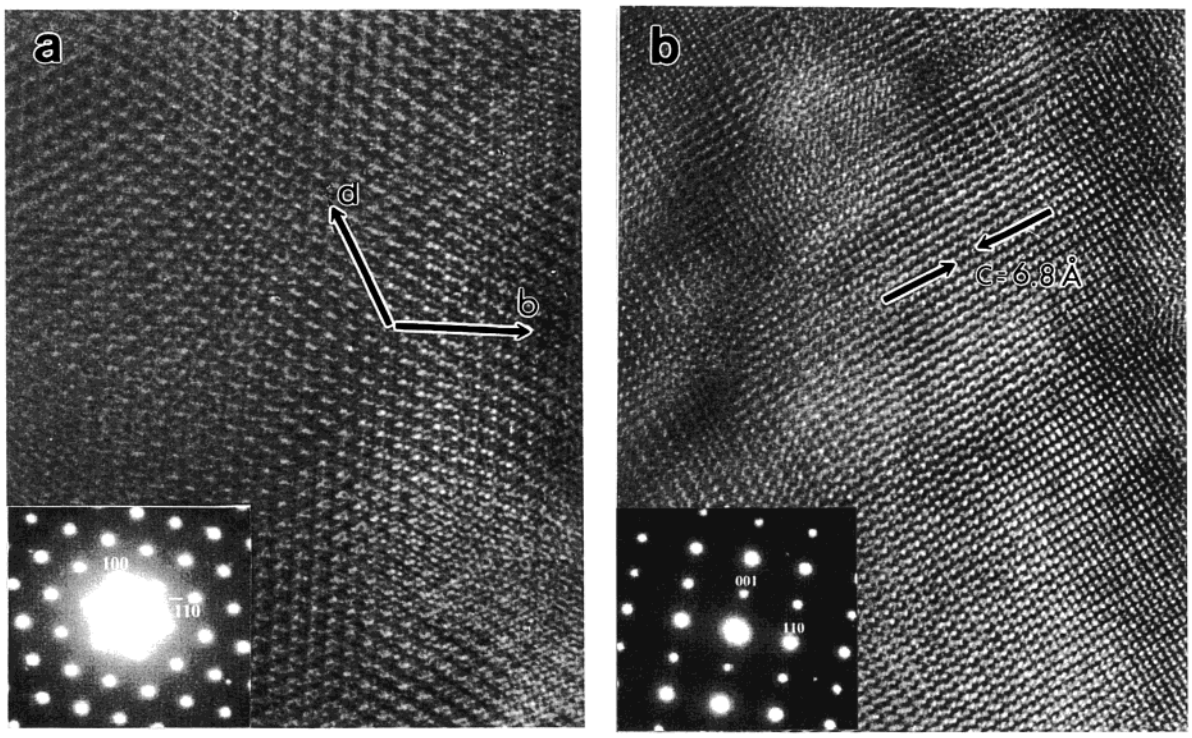

Figure 6. ED patterns and HRTEM micrographs for the $Ca_8La_2(PO_4)_6O_2$ sample along different zone axes: (a) [001] and (b) [−110].

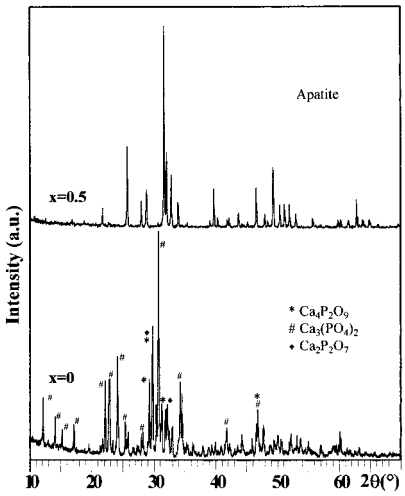

Figure 7. XRD patterns corresponding to series B samples.

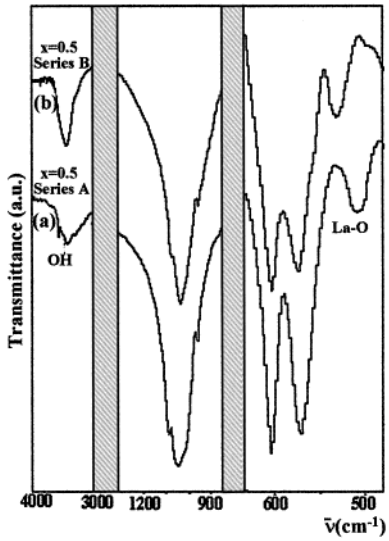

Figure 8. FTIR spectra corresponding to sample with $x = 0.5$: (a) series A and (b) series B.

composition do not decompose, showing an apatite-type single phase for all the composition range.

The Rietveld refinement of XRD data of series B samples shows that, again, La(III) ions are introduced only in the Ca(2) sublattice, that is, the synthesis conditions do not modify the preferential substitution of lanthanum for this position.

The FTIR spectra of the samples with lanthanum of series B give similar patterns to these observed in series A samples for $x \geq 0.8$ (see Figure 5c). In any case, the bands associated with hydroxyl groups were observed. Only absorption bands corresponding to vibrational modes of phosphate groups and an absorption band at 523 cm^{-1}, corresponding to the La−O bond, are observed in all the samples. If we compare the FTIR spectra of samples belonging to series A and B, we can see that only spectra corresponding to $x = 0.5$ are different. Figure 8 shows FTIR spectra corresponding to the sample with $x = 0.5$ for series A and B. When the sample with a lanthanum content equal to 0.5 was synthesized at 1200 °C (series A), the FTIR spectrum shows an absorption band at 3570 cm^{-1}, corresponding to an OH stretching band, and the La−O band appears at 505 cm^{-1} (Figure 8a). In this same composition treated at 1450 °C (series B) no OH bands were observed and the band corresponding to the La−O bond is displayed at 523 cm^{-1} (Figure 8b). These data seem to confirm our suggestion that in series A the shift of the La−O band at 505 cm^{-1} could be related with the existence of a hydrogen bond between OH^- and O^{2-} in the channels. These results show that the increase of the temperature led to a complete loss of OH^- ions, which are transformed in O^{2-}, keeping the apatite

structure. Then, in series B, when the samples were subjected to a final treatment at 1450 °C (120 h) (1) the sample without La decomposes to $Ca_3(PO_4)_2$, $Ca_2P_2O_7$, and $Ca_4P_2O_9$; and (2) when La is introduced into the structure, the phase does not decompose, even when just 5% of La is substituted. Now, all the samples correspond to an oxyapatite phase and the stoichiometry, in the entire composition range, can be described as

$$Ca_{10-x}La_x(PO_4)_6O_y\square_{y-x};\quad y = 1 + x/2;\quad 0.5 \le x \le 2$$

Taking into account the results obtained in both series, we can conclude that in series A, for $x = 0$, the composition of the sample corresponds to $Ca_{10}(PO_4)_6(OH)_{2-2y}O_y\square_y$, $y < 1$. The preparation of the dehydration product, i.e., $Ca_{10}(PO_4)_6O$, $y = 1$, needs very rigid conditions,[12] and its formation has been described as an intermediate product in the sintering process of apatites for orthopedic use[11] or due to the electron microscope beam.[24] However, the oxyapatite formed is very reactive and undergoes a rehydration,[12] leading in all cases to an oxy-hydroxyapatite phase. At high temperatures, around 1450 °C, it decomposes[23] according to the results obtained in this work for series B.

When La(III) is introduced in the OHAp structure, it is located in the Ca(2) position, independent of the compositional range or thermal treatment, keeping the apatite-type structure. To introduce higher lanthanum contents, it has been necessary to increase the synthesis temperatures and, consequently, more OH^- ions must be lost, by both the temperature effect and the introduction of a cation of higher valence. In series A, the sample that needed the lowest thermal treatment was for the $x = 0.5$ composition. For this sample, some OH^- ions remain in the structure, either because not all the OH^- ions were lost in this treatment or due to formation of a reactive oxyapatite. However, in series B, when the sample was synthesized at higher temperatures, all the OH^- ions were transformed, and the apatite obtained, $Ca_{9.5}La_{0.5}(PO_4)_6O_{1.25}\square_{0.75}$, is stable and nonreactive and does not decompose.

When more lanthanum is introduced into the structure, the apatite phase is stable and no differences were observed as a function of synthesis conditions. Then, for a lanthanum content $x \ge 0.8$, stable oxyapatites with a composition $Ca_{10-x}La_x(PO_4)_6O_y\square_{y-x}$, $y = 1 + x/2$, were obtained in both series.

The results show the possibility of stabilization of an apatite-type structure, without OH^- ions and with numerous anionic vacancies, for oxygen contents higher than one. This fact is possible by the introduction of a trivalent cation with a preferential substitution at the Ca(2) position in the hydroxyapatite.

Acknowledgment. We acknowledge the financial support of CICYT (Spain) through Research project MAT99-0466.

CM001117P

(24) Henning, P. A.; Landa-Cánovas, A. R., Kristin-Larsson, A.; Lidin, S. *Acta Crystallogr*. **1999**, *B55*, 170.